# Supplementary Information

# Redox-mediated conversion of atomically dispersed platinum to sub-nanometer particles

Yaroslava Lykhach,[a]* Alberto Figueroba,[b] Tomáš Skála,[c] Tomáš Duchoň,[c] Nataliya Tsud,[c] Marie Aulická,[c] Armin Neitzel,[a] Kateřina Veltruská,[c] Kevin C. Prince,[d] Vladimír Matolín,[c] Konstantin M. Neyman,[b,e]* Jörg Libuda[a,f]*

[a]Lehrstuhl für Physikalische Chemie II, Friedrich-Alexander-Universität Erlangen-Nürnberg, Egerlandstrasse 3, 91058 Erlangen, Germany

[b]Departament de Ciència dels Materials i Química Física and Institut de Química Teòrica i Computacional, Universitat de Barcelona, c/ Martí i Franquès 1, 08028 Barcelona, Spain

[c]Charles University, Faculty of Mathematics and Physics, Department of Surface and Plasma Science, V Holešovičkách 2, 18000 Prague, Czech Republic

[d]Elettra-Sincrotrone Trieste SCpA and IOM, Strada Statale 14, km 163.5, 34149 Basovizza-Trieste, Italy

[e]ICREA (Institució Catalana de Recerca i Estudis Avançats), Pg. Lluís Companys 23, 08010 Barcelona, Spain

[f]Erlangen Catalysis Resource Center, Friedrich-Alexander-Universität Erlangen-Nürnberg, Egerlandstrasse 3, 91058 Erlangen, Germany

*yaroslava.lykhach@fau.de; joerg.libuda@fau.de; Fax: +49 9131 8528867

*konstantin.neyman@icrea.cat; Fax +34 93 40 21 231

**S1. Sn deposition on Pt−$CeO_2$ film in an oxygen atmosphere**

The Sn 4d and Pt 4f spectra obtained from the 10% Pt−$CeO_2$ film following the Sn deposition in an oxygen atmosphere are shown in Figure S1a and S1b, respectively. The Pt 4f spectrum obtained from 10% Pt−$CeO_2$ film prior to Sn deposition (bottom trace, Figure 1b) contains a doublet at 73.0 eV (Pt $4f_{7/2}$) associated with $Pt^{2+}$ species.

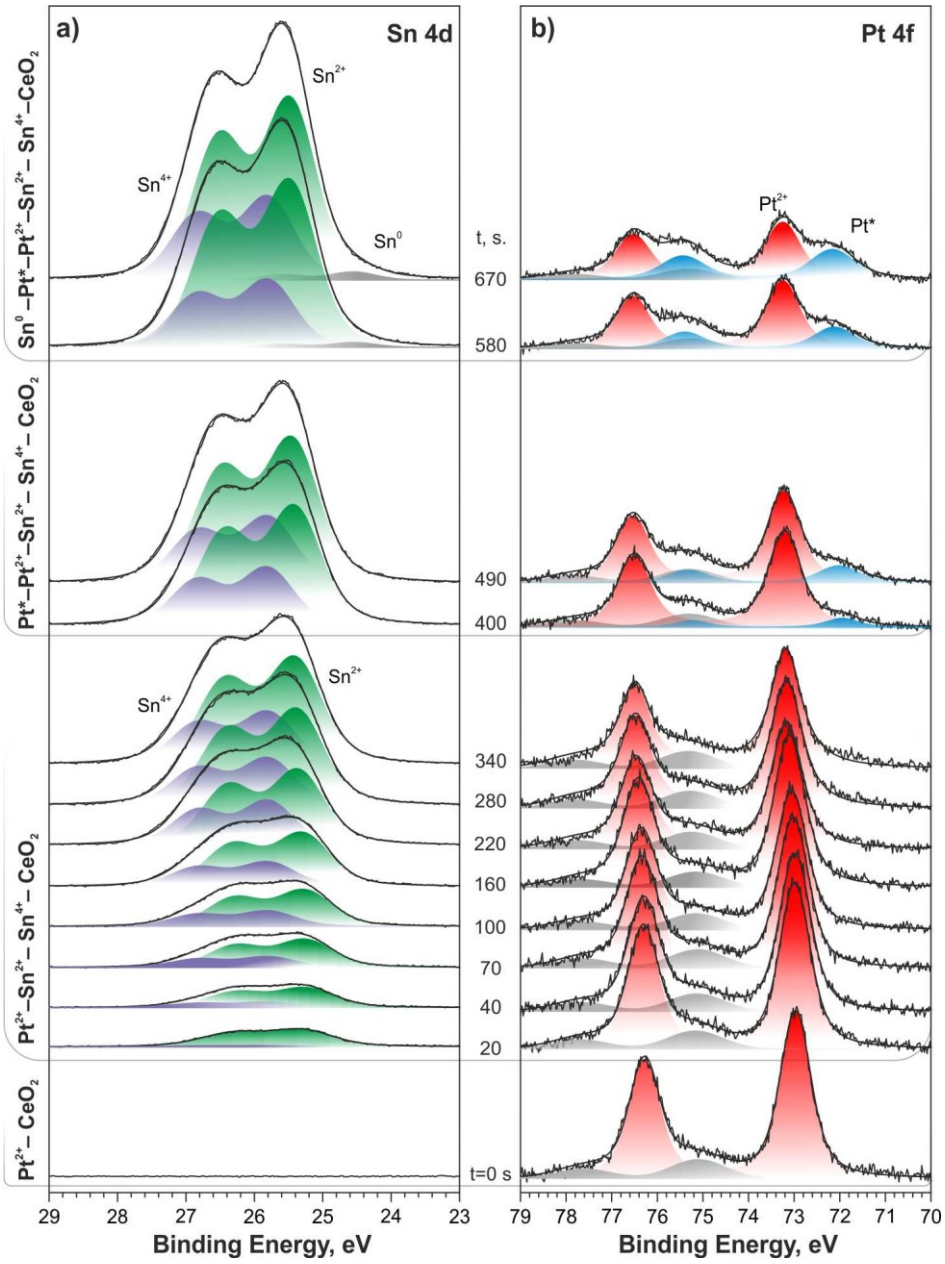


**Figure S1.** Sn 4d (a) and Pt 4f (b) spectra obtained from 10% Pt−$CeO_2$ film during stepwise Sn deposition at 300 K in $O_2$ atmosphere. The spectra were obtained with photon energies of 60 eV (Sn 4d) and 180 eV (Pt 4f).

Additionally, a minor contribution from the underlying Cu(111) substrate associated with the Cu 3p core level emerges at 75.0 eV (Cu $2p_{3/2}$).

The deposition of Sn under an oxygen atmosphere gives rise to two doublets in the Sn 4d spectra at 25.3 eV ($4d_{5/2}$) and 25.8 eV ($4d_{5/2}$). The corresponding peaks were assigned to $Sn^{2+}$ ions in a Sn−Ce oxide and $Sn^{4+}$ ions in $SnO_2$ or $Ce_2Sn_2O_8$ phases.[S1-3] Both peaks grow in intensity as a function of the Sn deposition time (Figure S1).

The development of the integrated Pt* intensities upon Sn deposition in UHV and in oxygen atmosphere is plotted in Figure S2 as a function of the integrated $Sn^{2+}$ intensity.

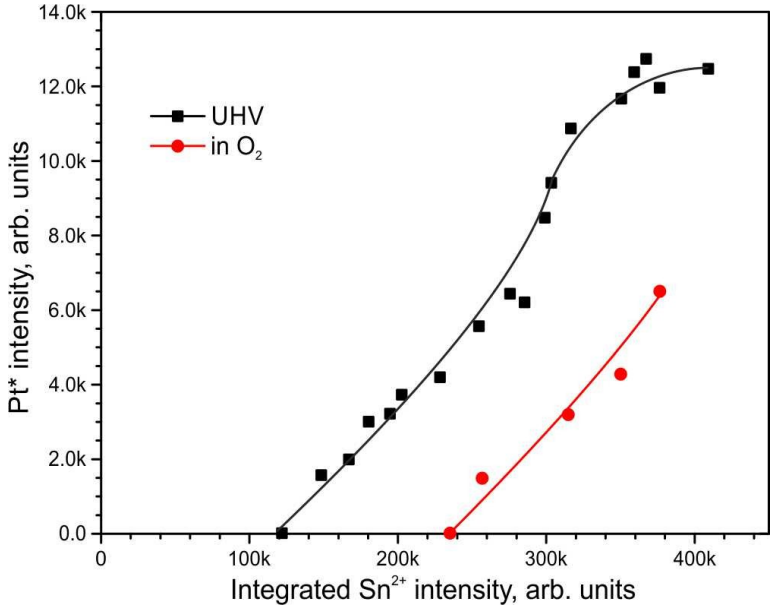


**Figure S2.** Development of the Pt 4f spectral contribution from ultra-small Pt* nanoparticles as a function of the integrated $Sn^{2+}$ intensity on a 10% Pt−$CeO_2$ film during stepwise deposition of Sn at 300 K in UHV (black squares) and in $O_2$ atmosphere (red circles).

**S2. The onset of $Pt^{2+}$ reduction and formation of sub-nanometer particles**

The circumstances of $Pt^{2+}$ reduction has been investigated with respect to the reduction degree of 10% Pt−$CeO_2$ film caused by Sn deposition under UHV.

Based on the concentrations of $Ce^{3+}$ and $Pt^{2+}$ species summarized in Table S1, we determined the corresponding number of $Ce^{3+}$ ions at the onset of the $Pt^{2+}$ reduction. We found that the emergence of 6 $Ce^{3+}$ centers triggers the reduction of one $Pt^{2+}$ species.

**Table S1.** Experimental estimation of the threshold ratio between the number of $Ce^{3+}$ centers formed and $Pt^{2+}$ ions reduced upon Sn deposition on the 10% Pt−$CeO_2$ film at 300 K in UHV.[a]

| t [s] | RER | Stoichiometry $Ce^{3+}/Ce^{4+}$ | $\Delta N(Ce^{3+})$ [$10^{18}$ $m^{-2}$] | $N(Ce^{3+})$ [$10^{18}$ $m^{-2}$] | $N(Pt^{2+})$ [$10^{18}$ $m^{-2}$] | $\Delta N(Pt^{2+})$ [$10^{18}$ $m^{-2}$] | $N(Ce^{3+})/\Delta N(Pt^{2+})$ |
|---|---|---|---|---|---|---|---|
| **0** | 0.12 | 0.0218 | 0 | 0 | 2.104 | | |
| **100** | 0.95 | 0.1719 | 0.9027 | 0.9027 | 2.098 | | |
| **120** | 1.10 | 0.1990 | 1.1951 | 1.5713 | 1.8392 | 0.265 | 5.93 |

[a]Columns from left to right: Sn deposition time; resonant enhancement ratio; $Ce^{3+}/Ce^{4+}$ concentration ratio; the change in the concentration of $Ce^{3+}$ cations; total number of $Ce^{3+}$ cations formed upon Sn deposition; $Pt^{2+}$ density; the number of reduced $Pt^{2+}$ species that corresponds to the number of formed Pt* species; ratio of the total number of $Ce^{3+}$ centers and the number of reduced $Pt^{2+}$ species (the number of formed Pt* species).

**S3. Profiling the depth distribution of Sn in the Pt−$CeO_2$ film**

The depth distribution of Sn in the 5% Pt−$CeO_2$ film has been investigated by means of the software for simulation of electron spectra for surface analysis SESSA 1.1.[S4] The analysis involves simulation of core level intensities based on the given structure and composition of the film. Thus, numerous model systems were assembled with respect to the Sn distribution in the 5% Pt−$CeO_2$ film. The intensities of the Sn 3d ($Sn^{2+}$ contribution), Ce 3d (a sum of $Ce^{4+}$ and $Ce^{4+}$ contributions), and O 1s core levels were simulated for each of the model. Then, the ratios of Sn/O and Ce/O intensities were determined and compared with the experimentally obtained values. In Figure S3, the experimental (symbols) and simulated (lines) Sn/O and Ce/O intensities are compared for two deposition times, t′ and t″.

The deposition of the corresponding amounts of Sn on the 5% Pt−$CeO_2$ film at both deposition times yielded exclusively $Sn^{2+}$ ions associated with the formation of Sn−Ce oxide, i.e. it did not involve the formation of metallic $Sn^0$ particles.

For the deposition time t′, the distribution of Sn was considered at the surface (models A-D) and in the bulk of 5% Pt−$CeO_2$ film without (E, F) and with (model G) subsequent intermixing with Ce cations (see Figure S3a).

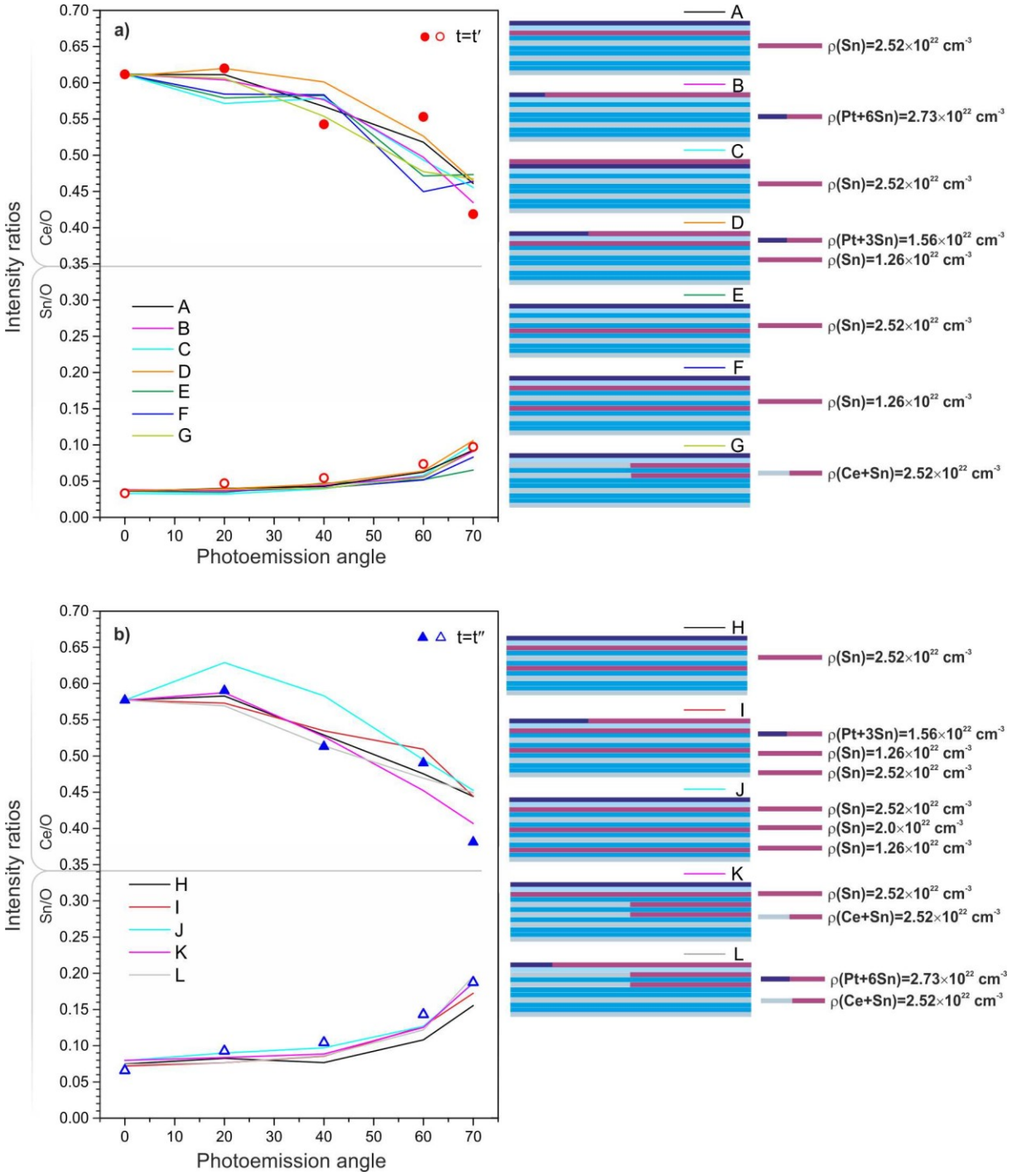


**Figure S3.** The ratio of the total intensities of Ce 3d to O 1s (Ce/O, top panel) and the ratio of $Sn^{2+}$ intensity in Sn 3d to O 1s (Sn/O, bottom panel) obtained at different photoemission angles from 5% Pt−$CeO_2$ film after the Sn deposition times t′ (a) and t″ (b) at 300 K in UHV. The corresponding models for the Sn-deposited 5% Pt−$CeO_2$ film are shown on the right.

The most distinct differences between the simulated and experimentally obtained Ce/O intensity ratios were observed for the models E-G concerned with the diffusion of Sn into the bulk. For these models, particularly incorrect trend in their angular functions was observed for the photoemission angles 60° and 70°.

Among the models A-D considering the Sn adsorption at the surface of 5% Pt−$CeO_2$ film, a good match was obtained with models A and B. In the model A, a Sn layer was placed below the low-density Pt−O layers. The model B considers Sn atoms to be adsorbed in the same layer with $Pt^{2+}$ species. Both models A and B yielded similarly good match between the simulated and experimental Ce/O ratios (see Figure S3a). In contrast, the model C obtained by placing a Sn monolayer on top of Pt film did not produce a satisfactory match between the simulated and experimental Ce/O ratios (see Figure S3a).

Finally, we considered a combination of both models A and B represented by the model D (see Figure S3a). The model D yielded a fairly good match between the simulated and experimental Ce/O ratios. Based on the comparison of the simulated and experimental angular function for Ce/O and Sn/O ratios, we conclude that Sn atoms will predominantly occupy the surface sites and are likely to diffuse under the low-density Pt−O layers. At the same time, diffusion of Sn into the deeper layers, e.g. below the Ce layers, is ruled out.

For the deposition time t″, we considered diffusion of Sn atoms into the bulk. Several models H-L were assembled followed by the comparison of the simulated and experimental angular functions of Ce/O and Sn/O ratios (see Figure S3b). The models H and I were built by combining the models A and E, and the models D and E, respectively. Thus, an additional Sn layer was inserted between the O−O layers below the first Ce layer. Additionally, the model J was built by inserting two Sn layers between the two O−O bulk layers of the model A, specifically, below the first and second Ce layers (see model J, Figure S3b). Here, we adjusted the Sn concentrations in the two bottom Sn layers to yield the best match with the experimental Sn/O ratios. No intermixing of Sn and Ce cations was considered in the models H-J.

Finally, the intermixing between the Sn and Ce cations was considered in the models K and L. Essentially, the model K was built on the basis of the model H by allowing the first Ce layer to intermix with bottom Sn layer at a ratio 1 to 1. Thus two mixed Ce/Sn layers were formed in the model K. Similarly, the model L was assembled based on the model B.

Overall, the best match between the simulated and experimental angular functions of Ce/O ratios was obtained with model K. Therefore, we conclude that at the deposition time t″, Sn atom will diffuse into the bulk and intermix with the Ce cations from the first Ce layer. Yet, diffusion of Sn below the second Ce layer is unlikely.

**S4. Temperature induced conversion of $Pt^{2+}$ species in the absence of metallic Sn**

The development of Sn 4d and Pt 4f spectra obtained from the 10% Pt−$CeO_2$ film after the last Sn deposition step under an oxygen atmosphere followed by annealing in UHV are shown in Figure S4a and S4b, respectively. The annealing of the 10% Pt−$CeO_2$ film promotes the reduction of $Pt^{2+}$ species. However, the reduction of $Pt^{2+}$ species is noticeably slower in comparison to the 10% Pt−$CeO_2$ film deposited with Sn under UHV. We relate the differences in the stabilities of $Pt^{2+}$ species on two samples to the presence of metallic $Sn^0$.

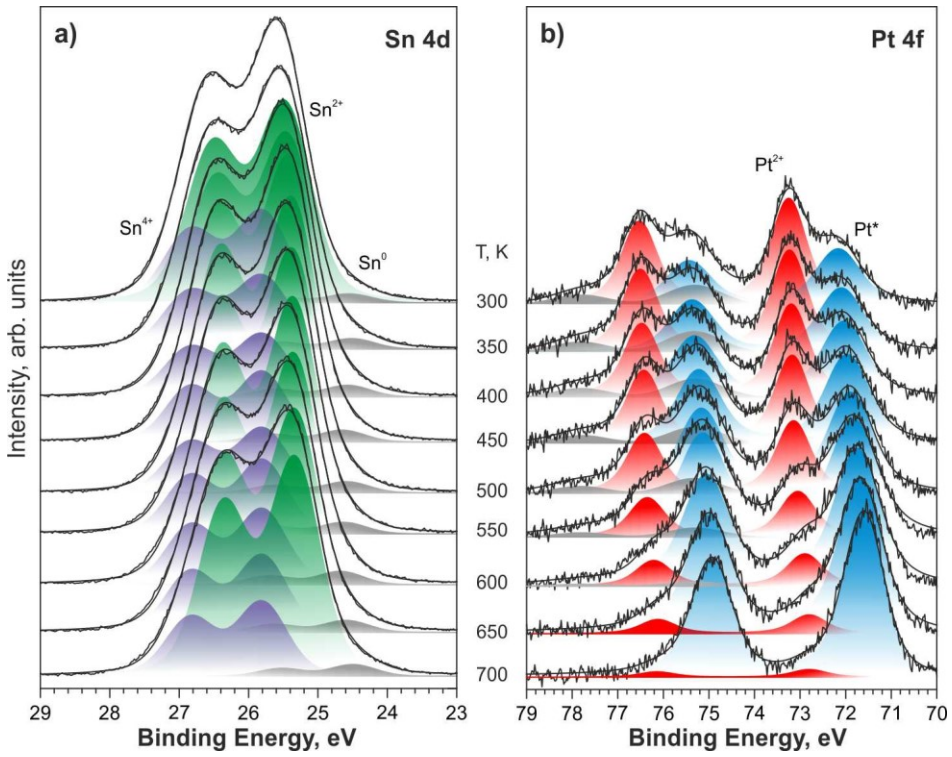


**Figure S4.** Sn 4d (a) and Pt 4f (b) spectra obtained during annealing of 10% Pt−$CeO_2$ after Sn deposition at 300 K in $O_2$ atmosphere. The spectra were obtained with photon energies of 60 eV (Sn 4d) and 180 eV (Pt 4f).

In particular, thermally triggered dissolution of $Sn^0$ into the bulk of the 10% Pt−$CeO_2$ film (see Section 3.4) results in the increase of $Ce^{3+}$ centers and facilitates reduction of $Pt^{2+}$ species. Therefore, in the absence of metallic $Sn^0$, reduction of $Pt^{2+}$ species requires higher annealing temperatures.

**S5. The degree of reduction of Ce cations in the 5% Pt−$CeO_2$ film controlled by Sn**

The Ce 3d spectra obtained from the 5% Pt−$CeO_2$ film before (t=0 s, 300 K) and after (t=t‴, 300 K) the Sn deposition in UHV at 300 K followed by annealing to 700 K in UHV (t=t‴, 700 K) are shown in Figure S5.

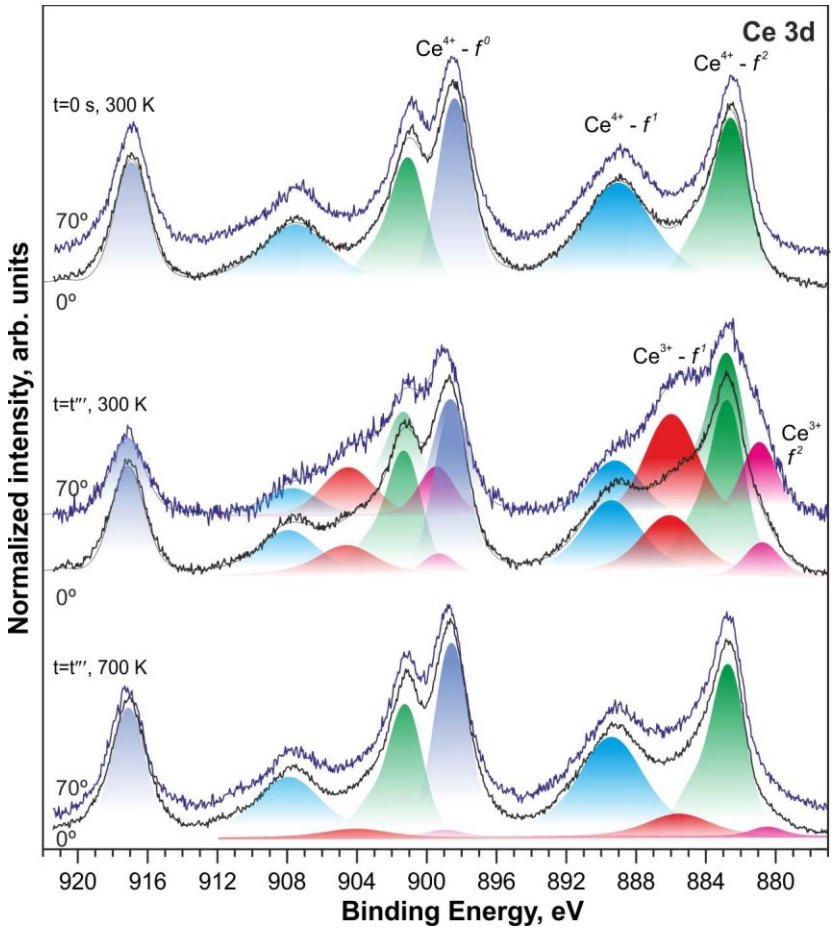


**Figure S5.** Ce 3d spectra obtained from 5% Pt−$CeO_2$ before (top) and after (middle) Sn deposition at 300 K followed by annealing to 700 K (bottom). The spectra were obtained at the photoemission angles 70° (dark blue) and 0° (black). The spectra were fitted with the multiple spectral contributions from $Ce^{4+}$ and $Ce^{3+}$ cations.

Here, the Ce 3d spectra obtained at the emission angles of 70º and 0º represent a chemical state of Ce cations at the surface and in the bulk, respectively. Prior to the Sn deposition, the Ce 3d spectra contain the contributions exclusively from the $Ce^{4+}$ cations at both photoemission angles. Three components at the binding energies of 882.5, 889.0, and 898.4 eV arise due to three different final states during photoemission related to the occupancy of the *f*-states in $Ce^{4+}$ cations. The deposition of Sn on the Pt−$CeO_2$ film in UHV results in the formation of $Ce^{3+}$ centers associated with the emergence of two additional doublets at 880.9 and 886.0 eV. The corresponding doublets arise from two different final states related to the occupancy of *f*-states in $Ce^{3+}$ centers. The comparison of the Ce 3d spectra at two photoemission angles, 70º and 0º, suggests higher concentration of $Ce^{3+}$ at the surface.

This observation is consistent with the formation of $Sn^{2+}$ preferentially close to the surface. As discussed in Section 3.3, the annealing of the 5% Pt−$CeO_2$ film after the deposition of Sn in UHV above 600 K resulted in the loss of Sn due to its dissolution in Cu(111). This process is accompanied by the re-oxidation of $Ce^{3+}$ cations both in the bulk and at the surface (see Figure S5, bottom spectra). This yielded sub-nanometer Pt particles supported on practically Sn-free nearly stoichiometric $CeO_2$ film.

**References**


S1. P. De Padova, M. Fanfoni, R. Larciprete, M. Mangiantini, S. Priori and P. Perfetti, *Surf. Sci.*, 1994, **313**, 379-391.

S2. A. Neitzel, Y. Lykhach, T. Skála, N. Tsud, V. Johánek, M. Vorokhta, K. C. Prince, V. Matolín and J. Libuda, *Phys. Chem. Chem. Phys.*, 2014, **16**, 13209-13219.

S3. T. Baidya, A. Gupta, P. A. Deshpandey, G. Madras and M. S. Hegde, *J. Phys. Chem. C*, 2009, **113**, 4059-4068.

S4. W. Smekal, W. S. M. Werner and C. J. Powell, *Surf. Interface Anal.*, 2005, **37**, 1059-1067.